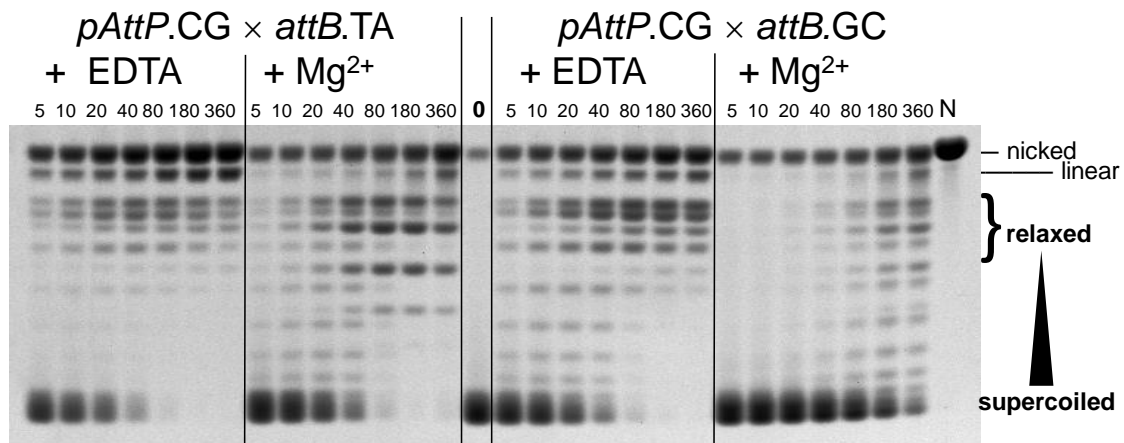


## **Supplementary Material**

### **“Crossover-site sequence and DNA torsional stress control strand interchanges by the Bxb1 site-specific serine recombinase”**

*Ross A. Keenholtz, Nigel D.F. Grindley, Graham F. Hatfull, and John F Marko*



**Figure S1. Kinetic analysis of supercoil relaxation by Bxb1 Int in ensemble reactions.** The agarose gel shown in Fig. 2C (after staining with ethidium bromide and imaging) was subjected to a further 3 hrs of electrophoresis. The bound ethidium differentially alters the migration behavior allowing all topologically closed plasmids (whether relaxed or supercoiled) to be separated from the nicked and linear species. It shows more clearly that the reacted portion of the substrate in the first panel is essentially fully relaxed at the earliest time points. For further details see Fig. 2 legend.

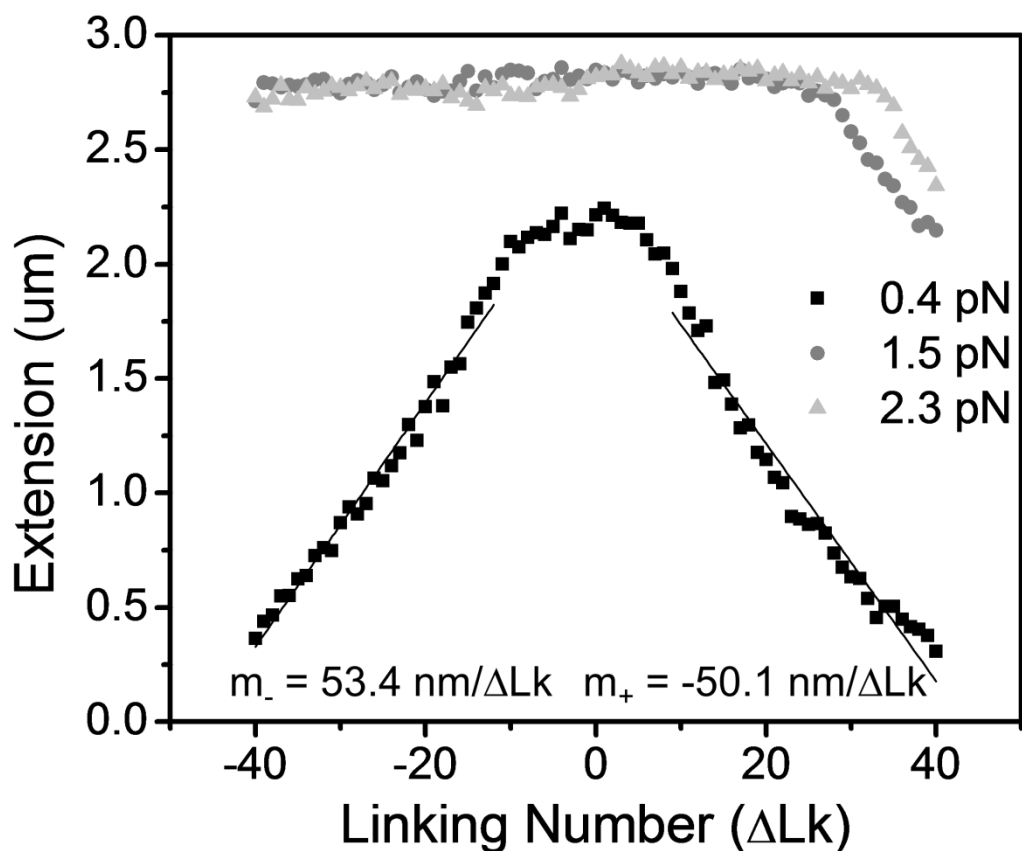


**Figure S2. DNA extension versus linking number.** Data are shown for pNG1175 and show the characteristic reduction of extension with increased  $|\Delta\text{Lk}|$  at different forces. For 0.4 pN, the extension near  $\Delta\text{Lk}=0$  varies slowly, but then varies nearly linearly for  $|\Delta\text{Lk}| > 10$ . In this regime plectonemic supercoils are being generated as  $|\Delta\text{Lk}|$  is increased, with an extension drop of approximately 50 nm per added unit of linking number. As relaxation occurs, these data are used to convert change in extension to rotation (measured in multiples of  $360^\circ$  turns). For larger forces, highly asymmetric curves are obtained, corresponding to torque-melting of DNA for  $\Delta\text{Lk} < 0$ .

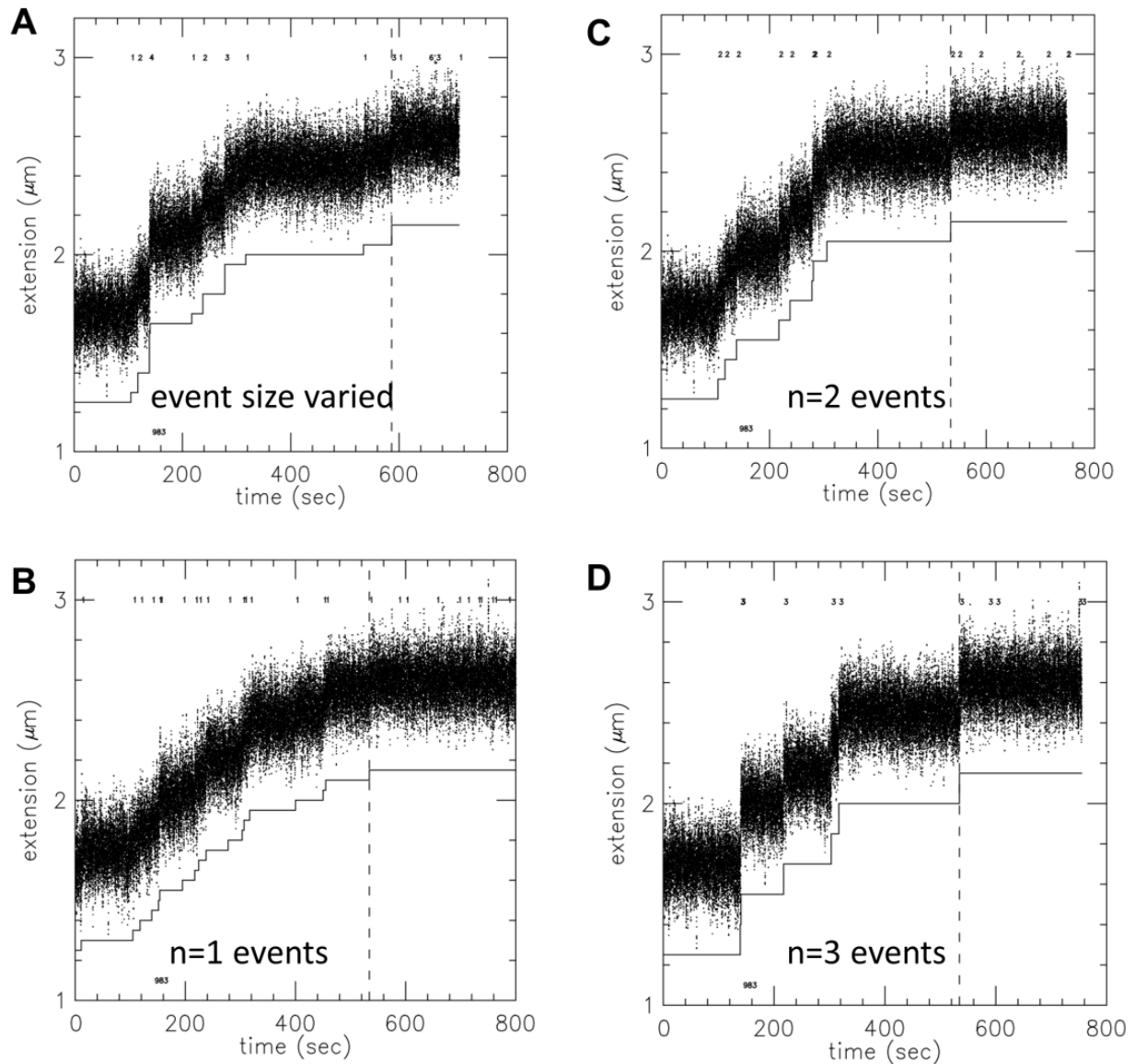


**Figure S3. Simulated relaxation trajectories.** We carried out simulations of relaxation of supercoiled DNA via a controlled rotation mechanism. A perfectly stepped relaxation (solid line) had Gaussian-distributed noise with standard deviation  $\sigma=0.105 \mu\text{m}$  and correlation time of 0.08 sec added to it, equal to experimentally measured values. Relaxations were assumed to give rise to extension changes of 50 nm per turn for  $\Delta Lk > 12$ ; for  $\Delta Lk < 12$ , the extension change was assumed to be zero. Relaxation runs were started from  $\Delta Lk = 30$  at time 0. Trajectories are shown for **A**: exponentially distributed step sizes similar to those observed experimentally; **B**: 50 nm ( $n=1$ ) steps only; **C**: 100 nm ( $n=2$ ) steps only; **D**: 150 nm ( $n=3$ ) steps only.

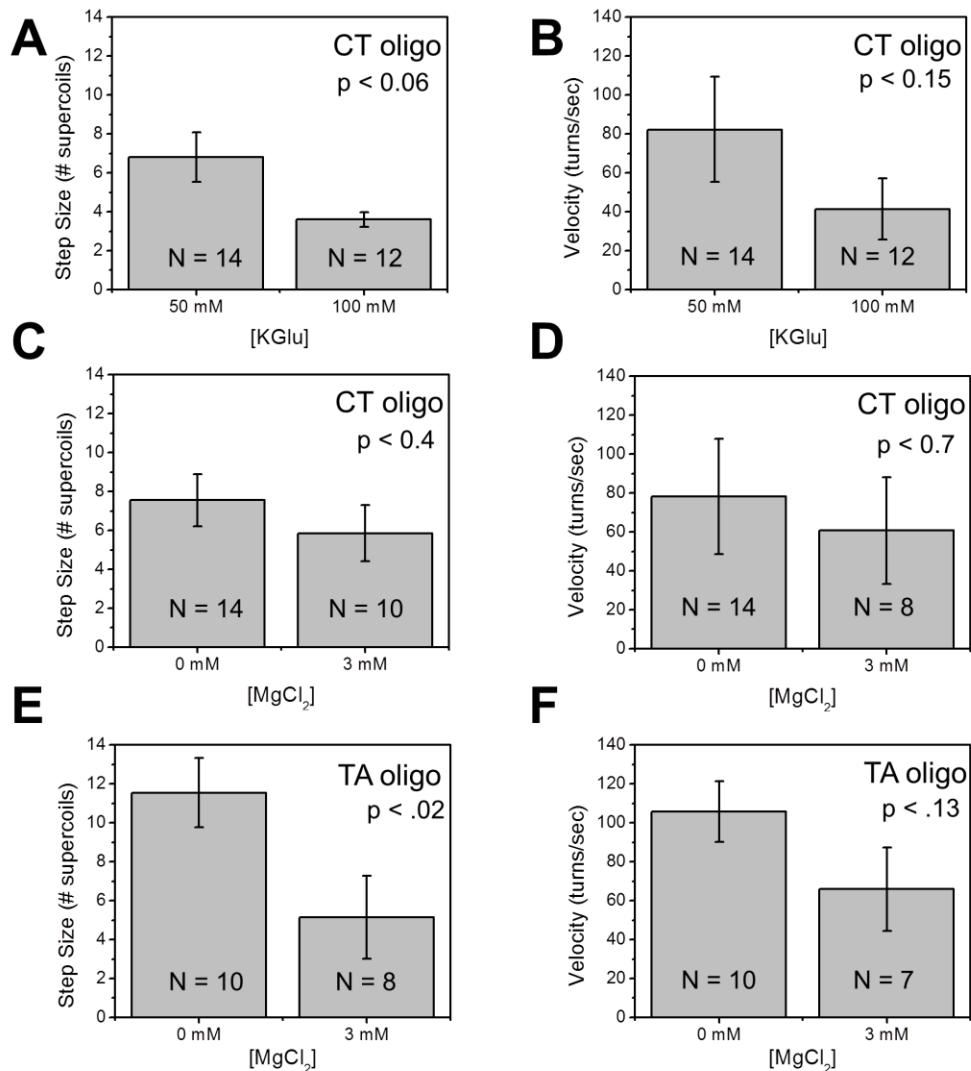


**Figure S4. Salt dependence of step size and velocity distributions.** For the intermediate-step-size case of the *attB*.CT oligomer, increasing the usual 50 mM KGlul concentration to 100 mM led to a decrease in step size (A) and velocity (B). By comparison, adding 3 mM Mg<sup>2+</sup> to the 50 mM KGlul reaction led to a small (not statistically significant) decrease in step size (C) and velocity (D). Adding 3 mM Mg<sup>2+</sup> to the 50 mM KGlul reaction with the .TA oligo however led to a more statistically significant decrease in step size (E) and velocity (F).

Sequence	Single-DNA-derived bp free energies (kcal/mol) $\Delta G^{\circ}_{25}$ [50 mM NaCl]	Unified nearest- neighbor bp free energies $\Delta G^{\circ}_{25}$ [50 mM NaCl]
5'-gCGc	-6.22	-6.53
gGCc	-5.62	-5.65
gCTc	-4.29	-4.63
gGTc	-3.96	-4.35
gTAc	-2.95	-3.27

**Table S1. Free energies of base pairing of the tetranucleotide spanning the crossover point and religation probabilities.** Base-pairing free energies were computed for the 4 bp region containing the crossover nucleotide predicted by a standard free energy model based on DNA melting (33) and by a single-DNA-experiment-based model (34). Both models predict an order of central dinucleotide stabilities  $TA < CT < CG$ . The free energy values shown were determined in aqueous solution and are only intended as a qualitative guide for free energy differences relevant to the Int synaptic complex.